JOURNAL OF Materials CHEMISTRY

Influence of fluoro substituents on the mesophase behaviour of banana-shaped molecules

J. P. Bedel,[a] J. C. Rouillon,[a] J. P. Marcerou,[a] M. Laguerre,[b] H. T. Nguyen[a] and M. F. Achard*[a]

[a]*Centre de Recherche Paul Pascal, Université Bordeaux I, Av. A. Schweitzer, 33600 Pessac, France. E-mail: achard@crpp.u-bordeaux.fr*
[b]*Institut Européen de Chimie et Biologie, Ecole Polytechnique-Université Bordeaux I-Université Bordeaux II- 16 Avenue Pey-Berland, 33607 Pessac, France*

Received 8th February 2002, Accepted 3rd May 2002
First published as an Advance Article on the web 13th June 2002

Three new series of bent-shaped five-ring liquid crystals, based on the ester of isophthalic acid as the central core and azomethine linkages, are presented. They differ by the number and the position of halogeno substituents on the outer rings. This lateral substitution strongly influences the type of mesophases formed. Calculations were performed to determine the modification of the distribution of charge along the different molecules.

Introduction

Until recently, the observation of ferroelectricity in liquid crystals, resulting in macroscopic electric polarization, was restricted to materials with chiral molecular structure. But in 1996, ferroelectricity was observed under an electric field in achiral compounds composed of bent molecules[1] and since this discovery, bent or ''banana-shaped'' liquid crystals have turned into a major field of research.

These materials form several new liquid crystalline phases, designated by the label B1–B8[2,3] and some of them exhibit interesting ferro-or antiferroelectric properties although the compounds are non-chiral. With exception of B3 and B4, all the B*n* mesophases present a lamellar organisation without in-plane order. B2, B6, B8 can be considered as the analogues of a ''monolayer'', ''intercalated'' and ''bilayer'' smectic respectively. B2 and B8 present an ''antiferroelectric type'' response. B5 presents a similar response. B1 and B7 correspond to more complex two-dimensional structures. In addition, for B7 type mesophases, a helical superstructure is probable but their complete structure is not solved. Note that this nomenclature remains preliminary and there are strong reasons to think that a ''B*n*'' appellation constitutes a group of mesophases, rather than an unique phase.

The bent shape of these molecules results from a central 1,3-phenylene or 2,7-naphthylene unit and compounds with five, six or seven aromatic (or heterocyclic) rings have been synthesised.[2] Nonetheless, most banana-shaped liquid crystals reported up to now correspond to five-ring mesogens with a 1,3-phenylene central unit as shown in Chart 1.

On the basis of this general formula, different chemical modifications can be considered and according to the available data, each alteration can lead to a change in or even to the loss of the liquid crystalline properties.

In particular, the influence of the nature, position and direction of the linking groups appears very strong. For example, the compounds in which the first ''B*n*'' phases were discovered[1] correspond to azomethine and carboxylic linkages with Y = -N=CH-, X = -COO-, X′ = -OOC-, Y′ = -CH=N- and the simple inversion of the sense of Y (-CH=N-) and Y′(-N=CH-) groups leads to the disappearance of these mesophases. We noted that connecting groups corresponding to an alternating distribution of the electronic density throughout the molecules favour the liquid crystalline properties.[4]

The influence of the alkyl or alkoxy terminal chains, which is often straightforward in calamitic mesogens, is not completely evident in banana-shaped compounds. Nevertheless, in homologous series, two or three different mesophases are observed depending on the length of the terminal chains.[2–11] In several series,[8,10,11] the short homologues present an intercalated smectic ''B6'' and/or a two dimensional ''B1 phase'' and the long chain derivatives show a switchable lamellar ''B2 phase''. Other systems present a more complex evolution of the polymorphism depending on the length or on the nature of the terminal chains.

The liquid crystalline properties of the banana-shaped compounds are also strongly influenced by the nature and position of the lateral substituents. Thus, modifying the initial structure[1] with a -$COCH_3$, -C_2H_5 or -C_6H_{13} group, attached at position 5 of the central phenyl ring (*i.e.* at the top of the molecule), the mesomorphic properties disappear.[2] With a chlorine[12] or a bromine[13] atom at position 4, the ''B2 phase'' is preserved. The introduction of a -CN group at position 4 gives rise to an unusual SA–SC–B2 sequence.[14] In contrast, the introduction of a methyl or a nitro group on position 2 of the central ring produces new mesophases (''B5'' for -CH_3[15] and ''B7'' for -NO_2[16]). These systematic studies were performed on the basis of the same series and underline the importance of the lateral substituents attached to the central ring.

The influence of substituents on the intermediate or outer rings has been less studied.[4,17–21] The first example of lateral substitution on the terminal phenyl rings (with a fluorine atom) was reported in a series with thiocarboxylic linkages:[4] up to

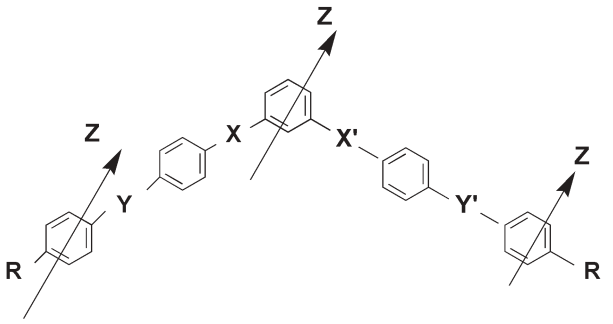

Chart 1 General formula of five-ring banana molecules.

 DOI: 10.1039/b201467j

four switchable banana phases, different from the referenced B*n* phases,[22] were observed whereas the unsubstituted compounds form nematic and smectic phases.

The goal of this paper is to systematically study the influence of different halogeno substitutions on the outer phenyl rings on the mesophase behaviour of banana-shaped compounds. The basic structure corresponds to a series previously published ("C*n*") which presents the same "B1" and "B2" phases[5] as the first reference series. The connecting groups are identical and the molecular structure was modified by introducing a fluorine atom at position 2 or 3 or two fluorine atoms at positions 2 and 3 on the external phenyl rings. In the three cases, complete homologous series with terminal alkoxy chains varying from 7 to 14 methylene groups have been synthesised.

Results and discussion

Materials

All the compounds were prepared following the general synthetic pathway shown in Scheme 1:

Isophthalaldehyde (0.1 mol) and 4-aminophenol (0.2 mol) were dissolved in boiling absolute ethanol in presence of a few drops of acetic acid. The solution was refluxed for 3 h. This condensation led to 1,3-bis[4-hydroxyphenyliminomethyl]benzene (compound **1**), which was recrystallized three times from a heptane–ethanol mixture.

To obtain the banana-shaped mesogens, the appropriate benzoic acid (compound **2**: 2 mmol) and compound **1** (1 mmol) were treated in dichloromethane with dicyclohexylcarbodiimide (2.2 mmol) and 4-dimethylaminopyridine as catalyst. The mixtures were stirred at room temperature for about 24 h. The products were recrystallized three times from ethanol–toluene and twice from toluene–heptane. Yields: 30–50%.

The transition temperatures and associated enthalpies are reported in Table 1. The phase assignment is based on complementary techniques, involving X-ray diffraction measurements optical observations, miscibility studies with known reference compounds and electro-optical analysis.

Substitution of a fluorine atom at position 2: D*n*F2 series

If a fluorine is attached at position 2 of the basic molecule a large decrease in both melting and clearing temperatures is observed and two types of mesophases exist depending on the number of carbon atoms in the chains.

On cooling from the isotropic liquid, the phase of the short homologues (n = 7–9) grows as dendritic nuclei which coalesce and give a mosaic texture (Fig. 1a). X-Ray patterns present a diffuse scattering at large angle and two incommensurate reflections in the small angle region suggesting a two-dimensional B1 phase. According to a B1 assignment, one can assume a rectangular lattice with a parameter "*c*" corresponding to the layer thickness (from the (002) reflection) and a parameter "*a*" (from the (101) reflection) attributed to the in-plane periodicity of the modulated phase. The X-ray data corresponds to a low value of the "*a*" parameter corresponding to a lattice involving few molecules.

The short chain homologues show neither polarisation current nor texture change under field as expected for a "B1" phase.

The longer homologues (n = 10–12 and 14) exhibit the same "B2" phase as in the non-substituted series. An example of the observed textures is given in Fig. 1b for the D11F2 compound.

The X-ray patterns of oriented samples (obtained by slow cooling of a drop of the isotropic liquid) correspond to tilted

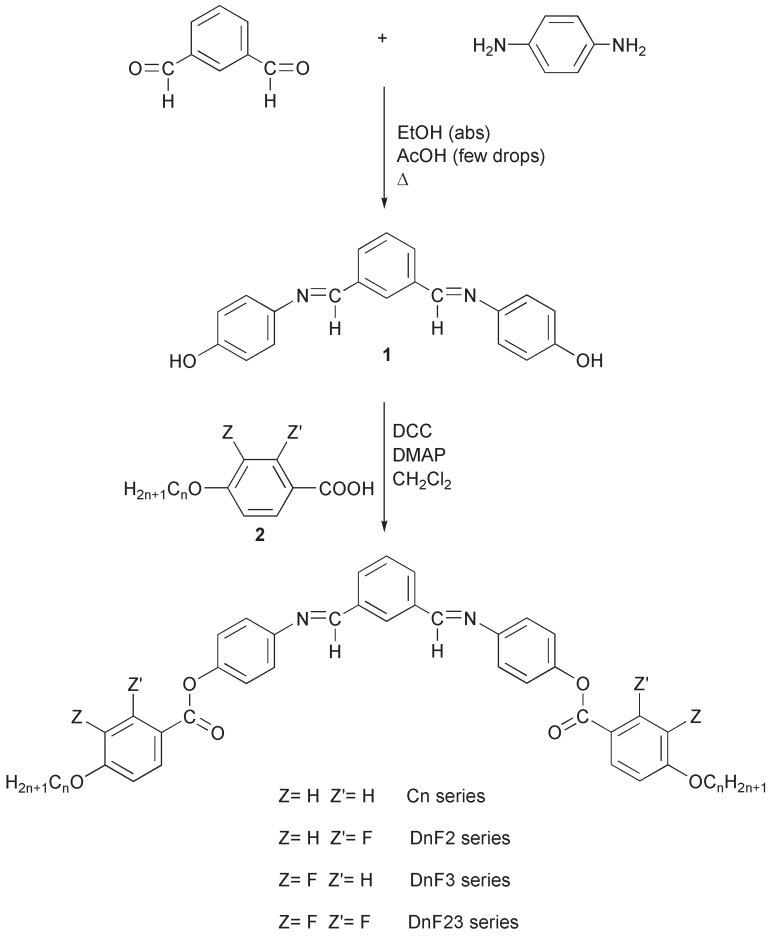

Scheme 1 Synthetic pathway used to obtain the C*n*, D*n*F2, D*n*F3 and D*n*F23 series of banana-shaped molecules. For each series, "*n*" corresponds to the number of carbon atoms in the terminal alkoxy chains and varies from 7 to 14.

Table 1 Transition temperatures (°C) and enthalpies (italics, kJ mol^{-1}) as a function of the carbon atoms number in the terminal chains (from DSC runs, increasing temperature, rate 5 °C min^{-1}). As usually observed in banana compounds, the enthalpy changes corresponding to the clarification transition are larger than for classical rod-like liquid crystals

n	C*n*					D*n*F2					D*n*F3					D*n*F23				
7	K	128.4 *28.7*	B1	152.9 *17.2*	I	K	120.4 *17.3*	B1	122.7 *13.3*	I	K	109.5 *26.9*	B1*x*	163.8 *23*	I	K	139.5 *25.6*	B1*x*	165.8 *19.4*	I
8	K	120.9 *29.2*	B1	153.5 *18.2*	I	K	103.5 *30.3*	B1	124.0 *17.1*	I	K	111.8 *33.4*	B1*x*	162.1 *23.4*	I	K	141.1 *22.7*	B1*x*	163.1 *20.3*	I
9	K	121.3 *32.0*	B1	147.2 *18.8*	I	K	100.7 *35.9*	B1	119.9 *16*	I										
9											K	112.8 *32.9*	$B7_{bis}$	160.3 *22.9*	I	K	138.7 *26.2*	$B7_{bis}$	162.0 *22.0*	I
10	K	120.4 *33.6*	B2	148.9 *20.1*	I	K	101.2 *30.5*	B2	123.8 *18.4*	I	K	111.5 *33.9*	$B7_{bis}$	158.9 *22.7*	I	K	137.6 *24.6*	$B7_{bis}$	161.8 *22.4*	I
11	K	117 *37.4*	B2	149.9 *21.1*	I	K	99.2 *30.4*	B2	126.1 *19.5*	I	K	111.7 *34.8*	$B7_{bis}$	158.3 *23.5*	I	K	137.0 *24.6*	$B7_{bis}$	162.3 *22.6*	I
12	K	115 *41.4*	B2	151 *22.3*	I	K	100.3 *23.5*	B2	129.2 *20.8*	I	K	111.0 *31.7*	$B7_{bis}$	157.0 *22.7*	I	K	136.2 *26.9*	$B7_{bis}$	162.5 *23.9*	I
13	K	116.7 *72*	B2	151.9 *23.2*	I						K	110.7 *48*	B2	156.6 *23*	I					
14	K	114.8 *68.5*	B2	150.4 *23.1*	I	K	97.0 *28.1*	B2	131.0 *22.2*	I	K	110.0 *50*	$B7_{bis}$	155.4 *22.7*	I	K	133.6 *25.8*	$B7_{bis}$	161.1 *23.8*	I

[a]K: crystalline phase, I: isotropic liquid. For liquid crystalline phase identification, see text. [b]The chloro derivatives D*n*Cl3 present the same mesophases as D*n*F3, but the transition temperatures are lowered: for example, K 82 °C $B7_{bis}$ 139 °C I for D12Cl3 compound.

smectics. The strong Bragg reflection in the small-angle region, with two harmonics reveals a layer structure (Fig. 2). The layer normal (meridian) is parallel to the drop axis. The diffuse scattering maxima in the wide-angle region indicate a liquid-like order within the layer and the tilt of the molecules with respect to the layer normal. This tilt angle (32°) appears significantly lower than for the non-substituted C*n* series (42°). Surprisingly, the layer spacing is also smaller in the D*n*F2 series than in the C*n* one (Table 2). This suggests a different arrangement of the molecules in the B2 phase, involving a larger interpenetration of the terminal chains in the fluorine substituted D*n*F2 compounds.

On applying a sufficiently high electric field (after a threshold of 8 V μm^{-1}), the long homologues react like a "B2 phase" with a two-peak polarisation response indicating the phase transitions under the application and the removal of the field between a non-polar and a polar phase (Fig. 3). The optical texture also changes after the threshold leading to two different figures with or without applied field. Note that there is no big difference between the textures at $-V$ and $+V$ unlike in a calamitic chiral smectic where the tilt angle flips from one direction to another.

To sum up, the introduction of a fluorine atom at position 2 on the outer phenyl rings of the banana-shaped molecules does not change the mesomorphism but causes a strong reduction of the mesophase stability in comparison with non-substituted compounds.

Substitution of a fluorine atom at position 3: D*n*F3 series[6]

At the opposite, the introduction of a fluorine atom at position 3 on the external phenyl rings increases the stability of the

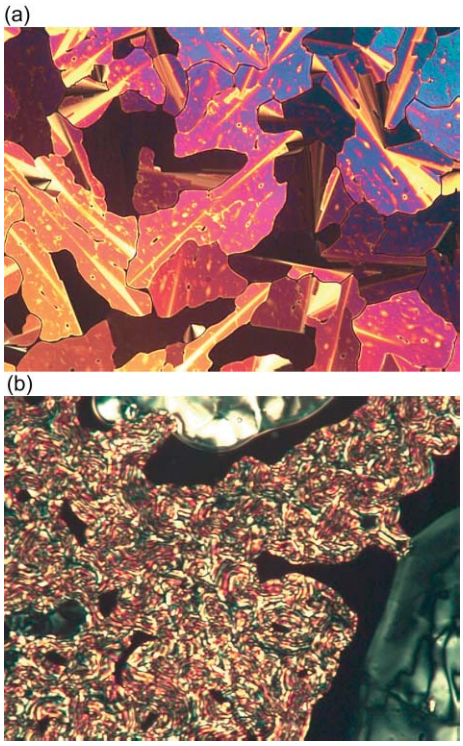

Fig. 1 a) Texture of the B1 phase of compound D9F2 (118 °C) b) Texture of the B2 phase of compound D11F2 (125 °C).

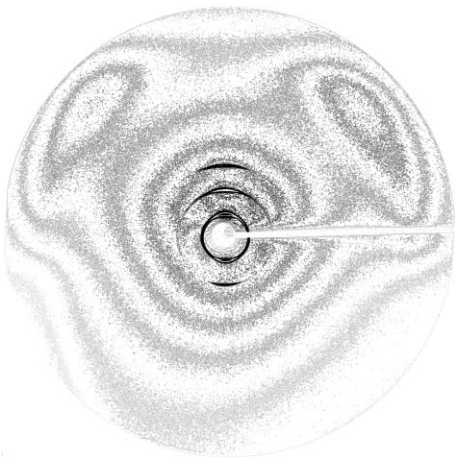

Fig. 2 X-Ray pattern of an oriented sample of D11F2 compound in the B2 phase.

Table 2 Linear increase of the layer spacing/Å *versus* the carbon number in the terminal chains. One can note a significant difference between the two series, which only differ by a fluorine substituent in position 2 of the outer phenyl rings

n	10	11	12	14
C*n* series	36.10	37.45	38.80	41.40
D*n*F2 series	33.40	34.90	36.10	38.75

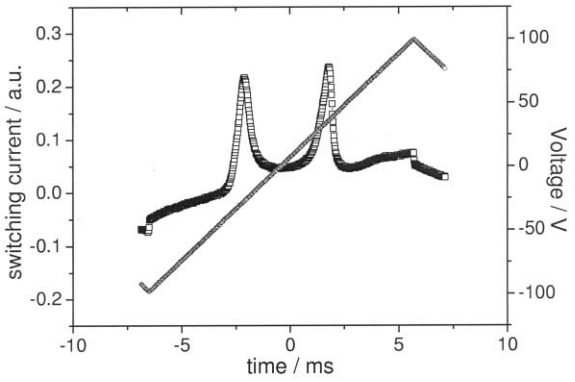

Fig. 3 Switching current response in the B2 phase of D12F2, obtained by applying a triangular voltage ($\pm$100 V; sample thickness 3.5 μm).

mesophase both by the decrease of the melting point and by an unusual enhancement of the clearing temperatures (see Table 1).

The short chain homologues (n = 7–8) exhibit a two-dimensional "B1x" phase which is structurally different from the two-dimensional B1 phase with a rectangular lattice observed in the non-substituted Cn compounds. The four incommensurate reflections in the small angle region are compatible with a rectangular centred lattice. Nevertheless, as for a B1 phase, the B1x mesophase shows again neither polarisation current nor texture change under electric field.

The longer homologues (n = 9 to 14) exhibit a " B7" variant, labelled "$B7_{bis}$" phase. As for the original "B7" observed in nitro-substituted compounds,[16] this $B7_{bis}$ phase presents a large variety of beautiful textures at the transition from the isotropic liquid and a complex X-ray pattern in the small angle region which excludes a simple layered organisation and suggests a two-dimensional structure. But in contrast to the original B7, it does have a polarisation response under applied field (Fig. 4) .

This response appears after a rather high threshold of about 10 V μm^{-1} and is constituted of only "one peak" per half period (*i.e.* a "ferroelectric type"). This means that the polarised phase created by the field has a long lifetime, so that it does not revert back to the zero-field non-polar phase when the field switches back and forth between $-V$ and V. As evidenced in Fig. 4 with a "triple plateau" voltage where V goes smoothly between three plateaux at $-$100 V, 0 V and +100 V, the polarisation has a lifetime greater than 10 ms and never vanishes in these conditions. It just rotates at constant modulus from $-P$ to $+P$ as in classical ferroelectric phases. When the field is switched off, the reverse phase transition to a non-polar phase takes place.

The polarisation value is between 300 and 380 nC cm^{-2} for the long homologues, the typical response time 100 μs and

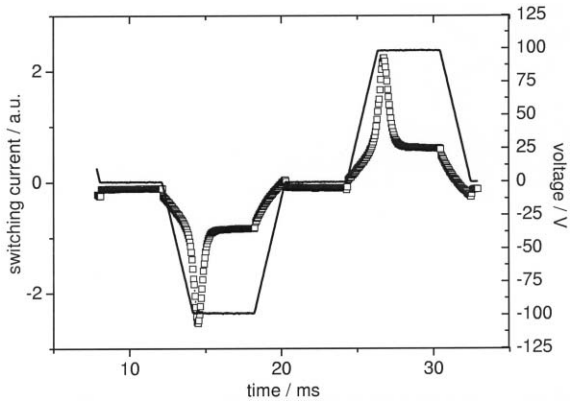

Fig. 4 Switching current response in the "$B7_{bis}$ phase" of D10F3, obtained by applying a modified triangular voltage ($\pm$100 V; sample thickness 5.4 μm; T = 120 °C).

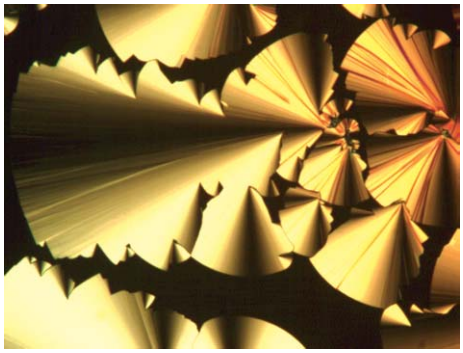

Fig. 5 Microscopic textures of the B1x mesophase of D8F23 compound (161 °C).

the threshold 10 V μm^{-1}. No significant variation is observed *versus* temperature in the mesophases.

Substitution of two fluorine atoms at positions 2 and 3: DnF23 series

By introducing two fluorine atoms at positions 2 and 3, the influence of the substitution on position 3 prevails and as for the DnF3 series, the "B1x" phase is observed for short homologues (n = 7, 8) and the long homologues present a "$B7_{bis}$" mesophase. In this DnF23 series, the clearing temperatures are higher than those of the non-substituted compounds but one can note in Table 1 the increase of the melting temperatures. Examples of the microscopic textures for both B1x and $B7_{bis}$ mesophases are given in Fig. 5a and 6.

The X-ray pattern of the B1x phase shows four reflections in the small-angle region (q = 0.078 Å^{-1}, 0.150 Å^{-1}, 0.163 Å^{-1} 0.307 Å^{-1} for D8F23) as for DnF3 compounds and a diffuse scattering at wide angles indicates the liquid like order of this mesophase.

In the same way, the long chain members of the DnF23 series present X-ray patterns similar to the DF3 series (Fig. 7).

The behaviour under electric field is similar to that of the DnF3 series. No response is observed for the B1x phase. For the $B7_{bis}$ phase, the field induces first the transition to a long-lived polar phase (*i.e.* a "one peak" response) after a threshold at about 12 V μm^{-1} as before. Nevertheless, contrary to the DnF3 series, at a second threshold of about 20 V μm^{-1}, this "one peak" response changes progressively in a few minutes into a "two peaks" one , indicating the transition with a short-lived polarisation (Fig. 8). The apparent polarisation is about 360 nC cm^{-2} for D11F3. This smooth transition is accompanied by a progressive change in the texture.

The examples shown in this paper give evidence of the subtle relationship between the chemical structure and mesomorphic properties of banana compounds. The introduction of a lateral fluorine substituent at position 3 on the terminal phenyl rings, which seems *a priori* a minor modification, leads to a drastic change in the mesomorphic behaviour since a two-dimensional "$B7_{bis}$" mesophase is observed instead of a layered "B2 phase". In the same way, a chlorine atom at position 3 or two fluorine atoms at positions 2 and 3 also induce a "$B7_{bis}$" mesophase, while a lateral fluorine substituent at position 2 preserves the "B2" phase.

It is clear that the molecular organisation of bent-shaped compounds results in a complex balance between the electrostatic interactions and the van der Waals interactions developed by the aliphatic chains. Thus the distribution of the electrostatic potential extrema† along the molecule will

†The electrostatic potential was calculated by VSS methods on lowest-energy conformers found after Monte-Carlo space conformation studies. Charge calculations were performed by using the MOPAC semi-empirical package with MNDO method.

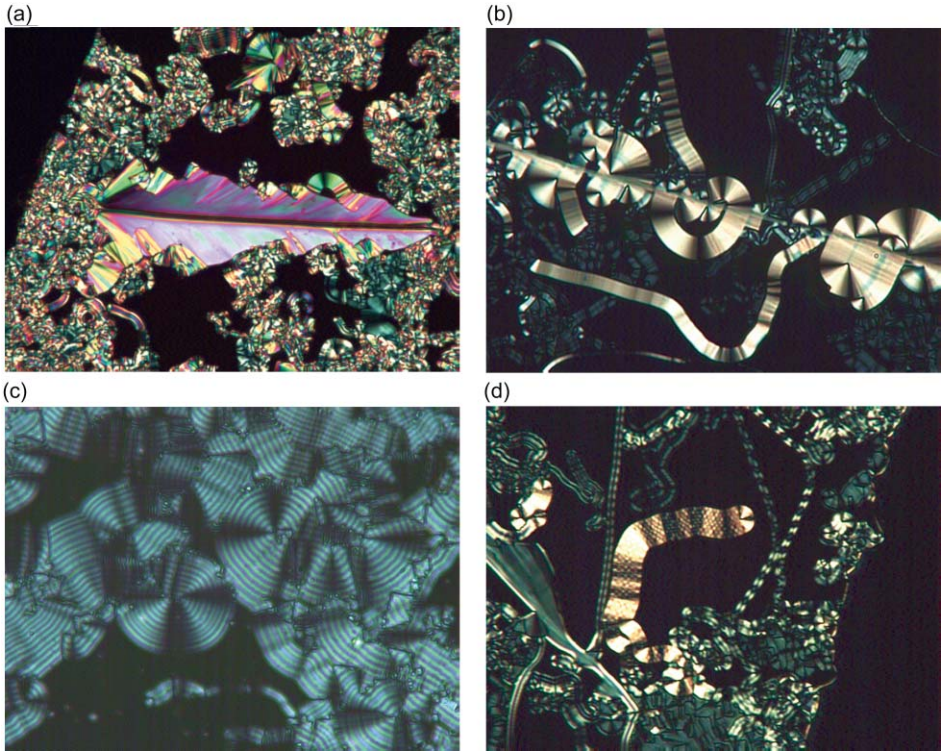

Fig. 6 Examples of the $B7_{bis}$ textures of the long homologues of the D*n*F23 series: a, ''banana-tree leaves''; b, different kinds of spiral germs indicating helicoidal structure; c, ribbons with equally spaced lines and d, two-dimensional periodic patterns.

Fig. 7 X-Ray pattern in the low-angle region of a non-oriented D9F23 sample: several reflections are seen ($q = 0.048$ Å^{-1}, 0.158 Å^{-1}, 0.302 Å^{-1} 0.322 Å^{-1}) but the structure cannot be determined without an oriented sample. Note that, increasing the chain length, the weaker reflections vanish and as for a smectic phase, an intense reflection with its first harmonic only is detected.

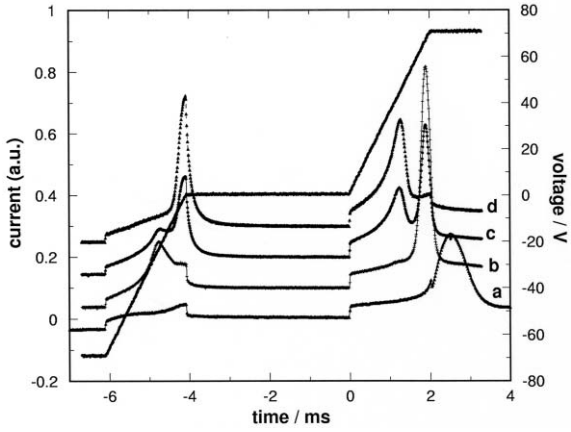

Fig. 8 Switching current response in the ''$B7_{bis}$ phase'' of D14F23, obtained by applying a modified triangular voltage (sample thickness 3.6 μm; $T = 136$ °C): a) $V = \pm 58$ V (below the second threshold), b), c), d) evolution with time at a voltage $V = \pm 71$ V corresponding to the second threshold.

strongly influence the molecular arrangement and the nature of the mesophases. Fig. 9 shows this repartition along a branch of the banana compounds. The presence of the halogeno substituents on the outer rings modifies the distribution of the potential extrema (Table 3): within the D*n*F3 and C*n* series, there appears a very contrasted pattern of negative extrema distributed along the branch, while there remains only a very deep negative extremum around the outer carboxylate moiety within the D*n*F2 series.

In the D*n*F2 series, the fluorine substitution at position 2 considerably increases the electrostatic potential and equalises

Table 3 Maximum values of the calculated electrostatic potential (kcal mol^{-1}) on the different parts of the molecule

Series Site	C*n*	D*n*F2	D*n*F3	D*n*Cl3	D*n*F2,3
Central ring	−5	−25	−3	−4	−24
CH=N	−26	−29	−24	−25	−27
Intermediate ring	−18	−29	−15	−8	−26
O	−22	−30	−20	−19	−28
C=O	−53	−54	−48	−50	−48
Outer ring	−5	−15	0	0	−7
O at the end of the branch	−22	−17	−30	−28	−25

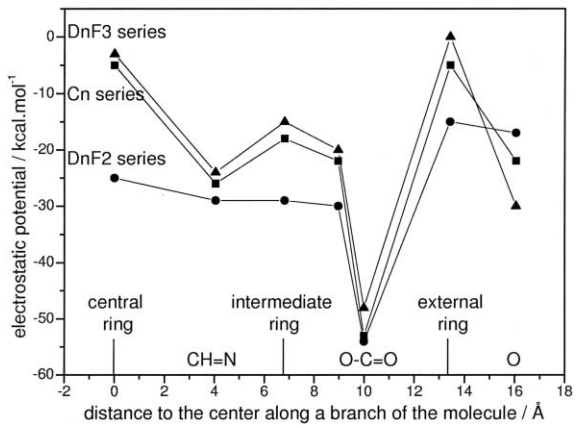

Fig. 9 Distribution of the electrostatic potential along a "branch" of banana compounds.

the negative charges from the centre of the molecule to the ester linkage. Thus, by comparison with the non-substituted C*n* series, the existence of a "B2 phase" does not depend on the repartition of the negative potential in the central part of the molecule. Moreover, the small difference of charges between the outer ring and the extremity favours the interpenetration of the aliphatic chains.

It is clear that the presence of a fluorine (or chlorine) atom at position 3 in the series D*n*F3 (or D*n*Cl3) only slightly reduces the electrostatic potential around the Schiff base and the ester group but largely reinforces the negative potential between the fluorine substituted phenylene group and the alkoxy group. The D*n*F23 series constitutes an intermediate case: an increase and an equalisation of the charges in the central part of the molecule is observed as for the D*n*F2 series, and the difference between the outer ring and the terminal group is kept as for the substitution at position 3.

These small differences are able to induce different molecular arrangements and thus different mesophases. It is obvious that the relationship between chemical structure and mesomorphic behaviour is a complex problem and that our understanding is still at an early stage.

3. Experimental

The thermal behaviour was investigated using a Perkin-Elmer DSC7 differential calorimeter. The optical textures of the mesophases were observed through a polarizing microscope (Leitz Diavert) equipped with a hot stage (FP-82HT) and an automatic controller (Mettler FP-90). Samples were observed on regular slide glass without any surface treatment.

X-Ray diffraction experiments were carried on a 18 kW rotating anode X-ray source (Rigaku-200) with use of a Ge(111) crystal as monochromator. The scattered radiation was collected on a two dimensional detector (Imaging Plate system from Mar Research, Hamburg). The samples were placed in an oven, providing a temperature control of 0.1 K.

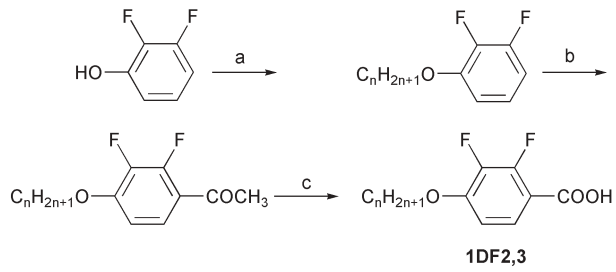

Scheme 2 *Reagents and conditions*: a: $C_nH_{2n+1}Br$, KOH, EtOH; b: CH_3COCl, $FeCl_3$, CH_2Cl_2; c: Br_2, NaOH, dioxane.

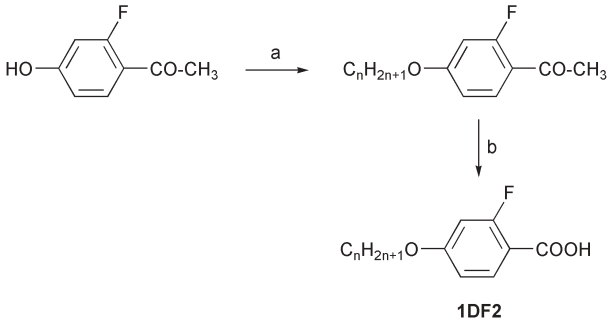

Scheme 3 *Reagents and conditions*: a: $C_nH_{2n+1}Br$, K_2CO_3, acetone; b: Br_2, NaOH, dioxane.

Oriented samples of the smectic phases were obtained by slow cooling of a drop of the isotropic liquid.

Electro-optical properties were studied using commercial cells (from E.H.C., Japan) with rubbed polyimide layer (but the surface treatment is not effective to make uniformly oriented cells).

Switching current was observed by applying a voltage-wave using a function synthesizer (HP 331 20A) and an high power amplifier (Krohn-Hite).

Synthesis of the benzoic acids (compounds 2):

The 2-fluoro-4-alkoxybenzoic acids were prepared according to the method shown in Scheme 2.[23]

The 3-fluoro-4-alkoxybenzoic acids (compounds **2**) were prepared according to the method shown in Scheme 3.[24]

The 2,3-difluoro-4-alkoxybenzoic acids were prepared according to the method shown in Scheme 4.[25]

Analytical data

1,3-Bis[4-(3-dodecyloxybenzoyloxy)phenyliminomethyl]benzene (compound C_{12}). ^{1}H NMR (200 MHz, $CDCl_3$) δ (ppm): 8.6 (2H, s, CH=N), 8.4 (1H, s, Ar-H), 8.13–8.18 (4H, d, Ar-H), 8.05–8.09 (2H, d,Ar-H), 7.6 (1H, t, Ar-H), 7.2–7.35 (8H, m, Ar-H), 6.95–7.00 (4H,d, Ar-H), 4.05 (4H, t, O-CH_2), 1.8–1.85 (4H, m, O-CH_2-CH_2), 1.25–1.5 (36H, m, CH_2), 0.85–0.92 (6H, m, CH_3).

IR (KBr) ν/cm^{-1}: 2920, 2851, 1726, 1606, 1509, 1472, 1289, 1254, 1193, 1170, 1086, 884, 852, 762, 683.

Elemental analysis: calculated: C: 78.03%; H: 8.07%; N: 3.14%. Found: C: 77.59%; H: 8.22%; N: 3.17%.

1,3-Bis[4-(2-fluoro-4-tetradecyloxybenzoyloxy)phenylimino-methyl]benzene (compound D_{14F2}). ^{1}H NMR (200 MHz,

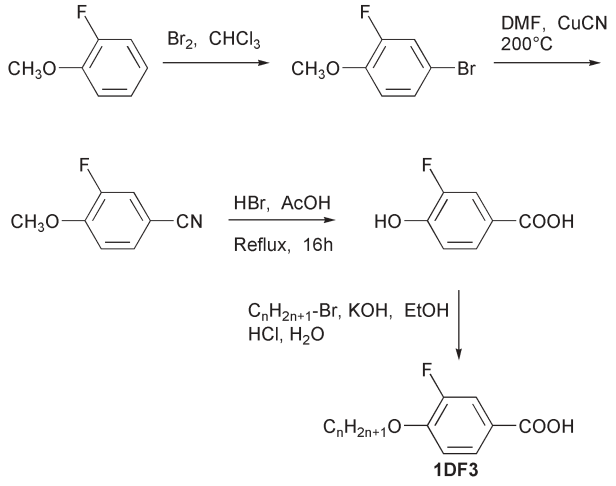

Scheme 4

$CDCl_3$) δ (ppm): 0.85–0.9 (m, 6H ,m, CH_3), 1.3 (m, 44H, $22CH_2$), 1.8 (m, 4H, 2 O-CH_2-CH_2), 4.05 (t, 4H, 2 O-CH_2), 6.65–6.8 (m, 4H, Ar-H), 7.25–7.35 (m, 8H, Ar-H), 7.6 (t, 1H, Ar-H), 8.1 (m, 4H, Ar-H), 8.4 (s, 1H, Ar-H), 8.6 (s, 2H, CH=N).

Elemental analysis: calculated: C: 75.61%; H: 7.93%; N: 2.84%; F: 3.86%. Found: C: 75.38 %; H: 7.98 %; N: 2.89 %; F: 3.59 %.

1,3-Bis[4-(3-fluoro-4-tetradecyloxybenzoyloxy)phenylimino-methyl]benzene (compound D_{14F3}). ^{1}H NMR (200 MHz, $CDCl_3$) δ (ppm): 0.85–0.9 (m, 6H, $2CH_3$), 1.25–1.5 (m, 44H, $22CH_2$), 1.8 (m, 4H, 2 O-CH_2-CH_2), 4.1 (t, 4H, 2 O-CH_2), 7.1 (t, 2H, Ar-H), 7.22–7.34 (m, 8H, Ar-H), 7.6 (t, 1H, Ar-H), 7.88–8.05 (m, 6H, Ar-H), 8.4 (s, 1H, Ar-H), 8.6 (s, 2H, CH=N).

Elemental analysis: calculated: C: 75.61%; H: 7.93%; N: 2.84%; F: 3.8 %. Found: C: 75.84%; H: 7.98%; N: 2.93%; F: 3.68%.

1,3-Bis[4-(2,3-difluoro-4-tetradecyloxybenzoyloxy)phenylimi-nomethyl]benzene (compound $D_{14F2,3}$. ^{1}H NMR (200 MHz, $CDCl_3$) δ (ppm): 0.85–0.9 (m, 6H, $2CH_3$), 1.25–1.5 (m, 44H, $22CH_2$), 1.8 (m, 4H, 2 O-CH_2-CH_2), 4.15 (t, 4H, 2 O-CH_2), 6.85 (m, 2H, Ar-H), 7.3 (m, 8H, Ar-H), 7.6 (t, 1H, Ar-H), 7.85 (m, 2H, Ar-H), 8.05 (d, 2H, Ar-H), 8.4 (s, 1H, Ar-H), 8.6 (s, 2H, CH=N).

References

1 T. Niori, T. Sekine, J. Watanabe, T. Furukawa and H. Takezoe, *J. Mater. Chem.*, 1996, **6**, 1231.
2 See for example: G. Pelzl, S. Diele and W. Weissflog, *Adv. Mater.*, 1998, **11**, 707 and references therein.
3 J. P. Bedel, J. C. Rouillon, J. P. Marcerou, M. Laguerre, H. T. Nguyen and M. F. Achard, *Liq. Cryst.*, 2001, **28**, 1285.
4 H. T. Nguyen, J. C. Rouillon, J. P. Marcerou and P. Barois, International Conference On Liquid Crystals, Strasbourg, 1999 (D2-O3); H. T. Nguyen, J. C. Rouillon, J. P. Marcerou, J. P. Bedel, P. Barois and S. Sarmento, *Mol. Cryst. Liq. Cryst.*, 1999, **328**, 177.
5 J. P. Bedel, J. C. Rouillon, J. P. Marcerou, M. Laguerre, M. F. Achard and H. T. Nguyen, *Liq. Cryst.*, 2000, **27**, 103.
6 G. Pelzl, S. Diele, A. Jakli, C. Lischka, I. Wirth and W. Weissflog, *Liq. Cryst.*, 1999, **26**, 135.
7 J. P. Bedel, J. C. Rouillon, J. P. Marcerou, M. Laguerre, H. T. Nguyen and M. F. Achard, *Liq. Cryst.*, 2000, **27**, 1411.
8 B. K. Sadashiva, V. A. Raghunathan and R. Pratibha, *Ferroelectrics*, 2000, **243**, 24.
9 A. Maranatha and B. K. Sadashiva, *Liq. Cryst.*, 2000, **27**, 1613.
10 J. C. Rouillon, J. P. Marcerou, M. Laguerre, H. T. Nguyen and M. F. Achard, *J. Mater. Chem*, 2001, **11**, 2946.
11 W. Weissflog, I. Wirth, S. Diele, G. Pelzl and H. Schmalfuss, *Liq. Cryst.*, 2001, **28**, 1603.
12 G. Pelzl, S. Diele, S. Grande, A. Jakli, C. Lischka, H. Kresse, H. Schmalfuss, I. Wirth and W. Weissflog, *Liq. Cryst.*, 1999, **26**, 401.
13 H. Dehne, M. Pötter, S. Sokolowski, W. Weissflog, S. Diele, G. Pelzl, I. Wirth, H. Kresse and S. Grande, *Liq. Cryst.*, 2001, **28**, 1269.
14 W. Weissflog, L. Kovalenko, I. Wirth, S. Diele, G. Pelzl, H. Schmalfuss and H. Kresse, *Liq. Cryst.*, 2000, **27**, 677.
15 S. Diele, H. Grande, H. Kruth, C. Lischka, G. Pelzl, W. Weissflog and I. Wirth, *Ferroelectrics*, 1998, **212**, 169.
16 G. Pelzl, S. Diele, A. Jakli, C. Lischka, I. Wirth and W. Weissflog, *Liq. Cryst.*, 1999, **26**, 135.
17 B. K. Sadashiva, H. N. Shreenivasa Murthy and Surajit Dhara, *Liq. Cryst.*, 2001, **28**, 183.
18 R. Amaranatha Reddy, B. K. Sadashiva and Surajit Dhara, *Chem. Commun.*, 2001, 1972.
19 G. Heppke, D. D. Parghi and H. Sawade, *Ferroelectrics*, 2000, **243**, 269.
20 C. K. Lee and L. C. Chien, *Ferroelectrics*, 2000, **243**, 231.
21 W. Weissflog, H. Nadasi, U. Dunemann, G. Pelzl, S. Diele, A. Aremin and H. Kresse, *J. Mater. Chem.*, 2001, **11**, 2748.
22 J. P. Bedel, J. C. Rouillon, J. P. Marcerou, M. Laguerre, H. T. Nguyen and M. F. Achard, submitted.
23 H. T. Nguyen, A. Babeau, J. C. Rouillon, G. Sigaud, N. Isaert and F. Bougrioua, *Ferroelectrics*, 1996, **79**, 33.
24 M. F. Nabor, H. T. Nguyen, C. Destrade, J. P. Marcerou and J. Twieg, *Liq. Cryst.*, 1991, **10**, 785.
25 S. M. Kelly, *Helv. Chim. Acta*, 1989, **72**, 594.